Adv. Theor. Appl. Mech., Vol. 3, 2010, no. 3, 139 - 149

Finite Element Study of Correlation between Intracranial Pressure and External Vibration Responses of Human Head

Zhaoxia Li [1] **and Yunhua Luo** [2]

Department of Mechanical & Manufacturing Engineering
University of Manitoba, Winnipeg, Canada, MB R3T 5V6

Abstract

In this paper, the correlation between intracranial pressure (ICP) and external vibration responses of the head was studied using finite element modeling. A two-dimensional finite element model of the head was constructed from magnetic resonance imaging (MRI) slice. The finite element model includes the skull, the cerebrospinal fluid (CSF) and the brain tissue. Material properties of the three components were obtained from the literature. A number of ICP values were selected from the normal ICP range. A series of finite element simulations were then conducted. In each of the simulations, one of the selected ICP values was applied to the finite element model. A harmless impact was exerted on one side of the head. External vibration responses were collected on the opposite side of the head. In all the simulations, the same impact was applied. The only factor that made a difference to vibrational responses was intracranial pressure. By comparing results obtained from all the simulations, it was found that all vibrational responses were related to intracranial pressure. However, some vibrational responses were more sensitive than the others to the change of intracranial pressure. The results from this study may be used as a base for developing a non-invasive procedure for evaluating intracranial pressure.

Keywords: intracranial pressure (ICP), finite element model, external vibration responses

[1]MSc student
[2]Corresponding author; E-mail: luoy@cc.umanitoba.ca

1 Introduction

With the use of protective helmets, more and more closed head injuries are reported [1, 2]. Usually a closed head injury is difficult to diagnose as the external symptoms are not obvious. Elevated intracranial pressure (ICP) is a common consequence of closed head injuries. However, it is difficult to evaluate without a reliable instrument. A timely treatment of elevated intracranial pressure is crucial to prevent permanent disability and death. Therefore, various methods and techniques have been developed for evaluating intracranial pressure. Most of them are invasive [3]. Invasive methods are reliable for obtaining absolute ICP. But they may cause infection due to their invasive feature. Non-invasive methods are more convenient and free of the concern of infection. However, they are not reliable for measuring absolute ICP. They are currently used mainly for monitoring purpose. It has been found in previous experimental studies [4, 5, 6] that an elevated intracranial pressure will cause changes in the external vibration responses of an animal head. This finding indicates that it is possible to establish a correlation between intracranial pressure and external vibration responses of human head. There is also a theoretical base for the correlation. That is the initial stress theory. An intracranial pressure produces an initial stress field in the skull, which in turn introduces a stress-related term in the skull stiffness. On the other hand, vibrational responses of the head are related to the stiffness of the skull.

Therefore, it is possible to develop a non-invasive procedure for evaluating ICP based on correlation between intracranial pressure and external vibration responses of the head. However, the correlation is affected by a number of factors, for example, the age, the gender, the ethnic group, and even the small anatomical differences from individuals. For the complex anatomical structure and the complicated material composition of the head, it is very difficult, if not impossible, to establish an analytical model for the correlation. For the anatomical differences between a human and an animal head, the correlation obtained from animal experiments can not be extended to human beings. Direct physical experiment on human beings may cause injury and it is not ethic either. In this paper, the possibility of using finite element modeling to establish the correlation is explored.

The main idea is briefly described as follows. As a first step, a two-dimensional finite element model of the head will be considered. The finite element model will be constructed from magnetic resonance images (MRI) of the head. The finite element model will include the skull, the cerebrospinal fluid (CSF) and the brain tissue. A number of ICP values will be selected from the normal ICP range. A series of finite element simulations will be conducted. In each of the simulations, one of the selected ICP value is applied to the finite element model. A harmless impact is exerted on one side of the head. External

vibration responses are collected on the opposite side. In all the simulations, the same impact is applied. The only factor that would make a difference to the vibrational responses is the applied intracranial pressure. For simplicity, it is assumed that mass density of the brain tissue will not change as intracranial pressure increases.

2 Physical Model and Finite Element Formulations

2.1 Physical model and governing equations

Magnetic resonance imaging (MRI) [7, 8] and magnetic resonance elastograpgy (MRE) [9, 10, 11] are non-invasive medical imaging technologies. The head medical images contain information of geometry and material properties of the head. Using a medical image processing software, a realistic physical model of the head can be constructed from the medical images. In this study, as a first step, a two-dimensional physical model is considered. Based on a rough segmentation, a two-dimensional head model consists of three major parts: the skull, the cerebrospinal fluid (CSF) and the brain tissue, see Fig. 1. In a living body, a pressure called intracranial pressure exists in the CSF. It is

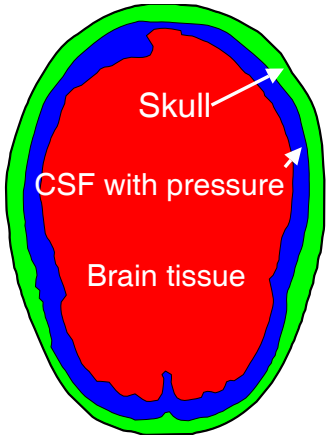

Figure 1: Two-dimensional physical model of the head

possible to construct a map of material properties for the brain tissue using medical images [12], so that material properties of the brain tissue can be described in a point-by-point way. However, in this study, the problem is simplified. The three parts of the head are treated as homogeneous materials. Their properties are obtained from the literature and listed in Table 1. The

Table 1: Material properties of human head components [13, 14, 15]

	Young's Modulus (MPa)	Bulk Modulus (MPa)	Poisson's Ratio	Mass Density (kg/m^3)
Skull	6650.0	-	0.220	2080
Brain	0.5581	2190	0.485	1040
CSF	0.1485	2190	0.499	1040

skull and the brain tissue are solid materials and the CSF is a fluid. Their behavior under mechanical excitations are governed by different mathematical equations. For the solid parts, if body force is not considered, the governing equation is [16]

$$\nabla \cdot \boldsymbol{\sigma} + \boldsymbol{\mu}\dot{\mathbf{u}} = \rho_s \ddot{\mathbf{u}} \tag{1}$$

where ∇ is the differentiation operator; $\boldsymbol{\sigma}$ is the vector containing the relevant stress components; ρ_s is the mass density of the solid parts; $\boldsymbol{\mu}$ is the matrix containing the damping coefficients of the solid materials; $\mathbf{u}$ is the displacement vector. A dot over a variable represents its derivative with respect to time.

The cerebrospinal fluid (CSF) is a slightly compressible fluid. Its density varies only by a small amount relative to its hydrostatic density and thus can be considered as constant. Under an impact, the relative motion between CSF and the solid parts is small and slow [18]. Therefore, convective effects of the CSF can be omitted. The CSF is considered as inviscid [1]. Therefore, stresses introduced by fluid viscous effects can be neglected. Under the above assumptions, the governing equation for the CSF part is [19]

$$\frac{1}{c^2}\frac{\partial^2 p}{\partial t^2} - \nabla^2 p = \mathbf{0} \tag{2}$$

In Eq. (2), $c = \sqrt{k/\rho_0}$ is the sound speed in CSF. In the above expression, k is the bulk modulus of CSF and ρ_0 is its hydrostatic density. p is the acoustic pressure and t is the time variable.

The interaction between CSF and the solid parts is introduced by boundary conditions at the fluid-solid interface [16]

$$\mathbf{n}^T \cdot \nabla p = -\mathbf{n}^T \cdot (\rho_0 \ddot{\mathbf{u}}) \tag{3}$$

In Eq. (3), $\mathbf{n}$ is the normal of a fluid-solid interface pointing to the fluid domain.

2.2 Finite element formulations

By following the standard finite element procedure [20, 16], finite element equations can be established from the governing equations in Eqs. (1), (2) and

(3). The finite element equation of the solid parts is

$$\mathbf{M}^{\mathrm{s}}\ddot{\tilde{\mathbf{u}}} + \mathbf{C}^{\mathrm{s}}\dot{\tilde{\mathbf{u}}} + \mathbf{K}^{\mathrm{s}}\tilde{\mathbf{u}} - \mathbf{Q}\tilde{\mathbf{p}} = \mathbf{0} \tag{4}$$

where $\mathbf{M}^{\mathrm{s}}$, $\mathbf{C}^{\mathrm{s}}$ and $\mathbf{K}^{\mathrm{s}}$ are, respectively, the mass, damping and stiffness matrices of the solid parts. A variable with an over tilde, for example $\tilde{\mathbf{u}}$, represents the discrete value of the variable at element nodes. $\mathbf{Q}$ is the fluid-solid coupling matrix. The expressions of the matrices are given in the following.

$$\begin{aligned} \mathbf{M}^{\mathrm{s}} &= \int_{\Omega_{\mathrm{s}}} \rho_s \mathbf{N}_{\mathrm{u}}^T \mathbf{N}_{\mathrm{u}} d\Omega, \qquad \mathbf{C}^{\mathrm{s}} = \int_{\Omega_{\mathrm{s}}} \mathbf{N}_{\mathrm{u}}^T \boldsymbol{\mu} \mathbf{N}_{\mathrm{u}} d\Omega \\ \mathbf{K}^{\mathrm{s}} &= \int_{\Omega_{\mathrm{s}}} \mathbf{B}_{\mathrm{u}}^T \mathbf{D} \mathbf{B}_{\mathrm{u}} d\Omega, \qquad \mathbf{Q} = \int_S \mathbf{N}_{\mathrm{u}}^T \mathbf{n} \mathbf{N}_{\mathrm{p}} dS \end{aligned} \tag{5}$$

In the above expressions, $\mathbf{N}_{\mathrm{u}}$ and $\mathbf{N}_{\mathrm{p}}$ contain, respectively, the shape functions of element displacements and pressure. $\mathbf{B}_{\mathrm{u}}$ is the strain-displacement matrix. S represents the fluid-solid interface in the head model.

The finite element equation for the CSF is

$$\mathbf{M}^{\mathrm{f}}\ddot{\tilde{\mathbf{p}}} + \mathbf{C}^{\mathrm{f}}\dot{\tilde{\mathbf{p}}} + \mathbf{K}^{\mathrm{f}}\tilde{\mathbf{p}} + \rho_0 \mathbf{Q}^T \ddot{\tilde{\mathbf{u}}} = \mathbf{0} \tag{6}$$

where $\mathbf{M}^{\mathrm{f}}$, $\mathbf{C}^{\mathrm{f}}$ and $\mathbf{K}^{\mathrm{f}}$ are the mass, damping and stiffness matrices related to CSF. Their expressions are provided in the following.

$$\mathbf{M}^{\mathrm{f}} = \int_{\Omega_{\mathrm{f}}} \mathbf{N}_{\mathrm{p}}^T \frac{1}{c^2} \mathbf{N}_{\mathrm{p}} d\Omega, \quad \mathbf{C}^{\mathrm{f}} = \int_S \mathbf{N}_{\mathrm{p}}^T \frac{1}{c} \mathbf{N}_{\mathrm{p}} dS, \quad \mathbf{K}^{\mathrm{f}} = \int_{\Omega_{\mathrm{f}}} \mathbf{B}_{\mathrm{p}}^T \mathbf{B}_{\mathrm{p}} d\Omega \tag{7}$$

In Eq. (7), $\mathbf{B}_{\mathrm{p}}$ contains the derivatives of $\mathbf{N}_{\mathrm{p}}$ with respect to the spatial variables.

Finite element equations in Eqs. (4) and (6) can be put together in one equation

$$\begin{bmatrix} \mathbf{M}^{\mathrm{s}} & \mathbf{0} \\ \rho_0 \mathbf{Q}^T & \mathbf{M}^{\mathrm{f}} \end{bmatrix} \begin{Bmatrix} \ddot{\tilde{\mathbf{u}}} \\ \ddot{\tilde{\mathbf{p}}} \end{Bmatrix} + \begin{bmatrix} \mathbf{C}^{\mathrm{s}} & \mathbf{0} \\ \mathbf{0} & \mathbf{C}^{\mathrm{f}} \end{bmatrix} \begin{Bmatrix} \dot{\tilde{\mathbf{u}}} \\ \dot{\tilde{\mathbf{p}}} \end{Bmatrix} + \begin{bmatrix} \mathbf{K}^{\mathrm{s}} & -\mathbf{Q} \\ \mathbf{0} & \mathbf{K}^{\mathrm{f}} \end{bmatrix} \begin{Bmatrix} \tilde{\mathbf{u}} \\ \tilde{\mathbf{p}} \end{Bmatrix} = \begin{Bmatrix} \mathbf{0} \\ \mathbf{0} \end{Bmatrix} \tag{8}$$

It should be noted that the finite element matrices in Eq. (8) are not symmetric. The Newmark method [20] is used for time integration in the above finite element equation.

3 Numerical Studies and Results

The normal range of intracranial pressure (ICP) is approximately between 3.75 $\sim$ 15 (mmHg) [3], or between 500 $\sim$ 2000 (Pa). To study correlation between

ICP and vibrational responses of the head, four ICP values, 500(Pa), 1000(Pa), 1500(Pa) and 2000(Pa), are selected from the above range. A series of finite element (FE) simulations are then conducted. In each of the FE simulations, one of the selected ICP values is applied to the cerebrospinal fluid (CSF) of the finite element model. The initial stress fields introduced in the skull and in the brain tissue by the applied intracranial pressure is obtained by a static finite element analysis. The stiffnesses of the finite element model contributed by the stress-free state and by the initial stress fields are computed. A harmless impact in the form of step impulse, as shown in Fig. 2(a), is exerted on one side of the head. The location of the impact is shown in Fig. 2(b). A transient analysis is then conducted based on the finite element equations in Eq. (8). External vibration responses are collected on the opposite side of the head.

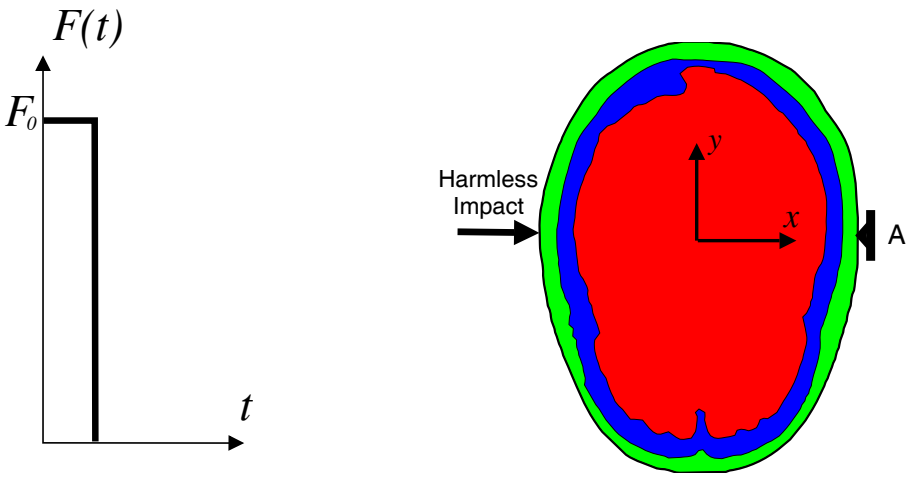

(a) (b)

Figure 2: (a) Harmless impact in the form of step impulse; (b) Locations for applying impact and for collecting vibrational responses

The location is marked by an 'A' in Fig. 2(b). In all the FE simulations, the same impact is applied. The only factor that makes differences to vibrational responses of the head is the applied intracranial pressure.

Peak values of commonly concerned vibrational responses, including displacement (u_x), velocity (v_x), acceleration (a_x), and effective strain (ϵ_e) at location 'A', obtained from the finite element simulations are listed in Table 2. The reason why only the x-direction components are studied is that they are the quantities that will be picked up by a sensor installed at the location. It can be observed from the results that the vibrational responses vary when the the intracranial pressure is changed. However, the magnitudes of the vari-

Table 2: Vibrational responses of the head under different ICP

ICP (Pa)	500	1000	1500	2000
Displacement (u_x, m)	7.77e-05	1.54e-04	2.31e-04	3.07e-04
Velocity (v_x, m/s)	8.68e-03	1.73e-02	2.58e-02	3.44e-02
Acceleration (a_x, m/s^2)	11.2	14.2	19.1	24.1
Strain (ϵ_x)	2.47e-06	4.20e-06	5.93e-06	7.66e-06
Fundamental freq. (Hz)	137.53	137.64	137.72	137.78

ations are not the same. The above observation confirms that a one-to-one correlation exists between ICP and a vibrational response. The normal range of a vibrational response corresponding to the normal ICP can be determined by finite element modeling. The obtained normal response range can be used to monitor and to evaluate ICP in clinic. One possible way is to compare the measured vibrational response against the normal response range. If the measured response falls in the normal response range, the ICP is normal. Otherwise it is abnormal. An even better way is to make correlation curves by producing more finite element simulation data. Once a vibrational response is measured, the corresponding ICP can be determined from the correlation curve.

In practice it is desired that even a small change in ICP can be reflected in a vibrational response. It requires that the vibrational response is sensitive to ICP change. To measure the sensitivity of a vibrational response to ICP change, the following sensitivity definition is introduced

$$\eta = \frac{\Delta w/w_u}{\Delta p/p_u} = \frac{(w_u - w_l)/w_u}{(p_u - p_l)/p_u} \tag{9}$$

where w represents a vibrational response; p is the intracranial pressure; subscripts u and l stand for, respectively, the upper and lower values of an increment in ICP or in the vibrational response. The sensitivities of the five vibrational responses listed in Table 2 are calculated using the above formula. The obtained sensitivities are provided in Table 3. From the results, it can be seen that displacement and velocity are the most sensitive to ICP change. For displacement and velocity, the correlation is approximately linear. Acceleration and effective strain are less sensitive to ICP change and the correlation is nonlinear. Fundamental frequency is the most insensitive to ICP change. This is due to fact that the skull is very stiff. The initial stress stiffness introduced by intracranial pressure is relatively very small. This phenomenon can be more clearly explained using the simple mass-spring system shown in Fig. 3. The natural frequency of the system is $f = \sqrt{k/m}$. If there is a

Table 3: Sensitivity of vibrational responses to ICP change

ICP change(Pa)	500-1000	1000-1500	1500-2000	Averaged
Displacement (u_x)	0.991	1.000	0.990	0.994
Velocity (v_x)	0.997	0.989	1.000	0.995
Acceleration (a_x)	0.423	0.770	0.830	0.674
Effective strain (ϵ_e)	0.824	0.876	0.903	0.868
Fundamental Freq.	0.0016	0.0017	0.0017	0.00167

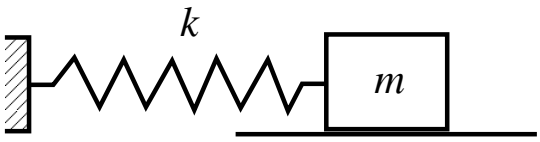

Figure 3: A single degree mass-spring system

change in the spring stiffness (δk), then the change in the natural frequency is $\Delta f = \sqrt{(k+\delta k)/m} - \sqrt{k/m}$. If δk is far less than k, then Δf would be very small.

A set of vibrational responses corresponding to ICP=1000(Pa) are shown in Fig. 4. It can be observed from the figures that the velocity and the acceleration gradually decay to zero. While the displacement and the effective strain do not go back to zero due to the initial stresses introduced by intracranial pressure.

4 Conclusions

In this paper, correlation between intracranial pressure (ICP) and external vibration responses of the head is studied using finite element modeling. A two-dimensional finite element model of the head is constructed from magnetic resonance imaging (MRI) slice. A number of ICP values are selected from the normal range of ICP. A series of finite element simulations are then conducted to obtain vibrational responses corresponding to the selected ICP. In all the simulations, the same impact is applied. The only factor that makes a difference to vibrational responses is the intracranial pressure. By studying the results obtained from the finite element simulations, it is found that all vibrational responses are related to intracranial pressure. The displacement, the velocity and the fundamental frequency have an approximately linear correlation with ICP. While the correlation of the acceleration and the effective strain with ICP is nonlinear. To measure how sensitive to ICP change a vibrational

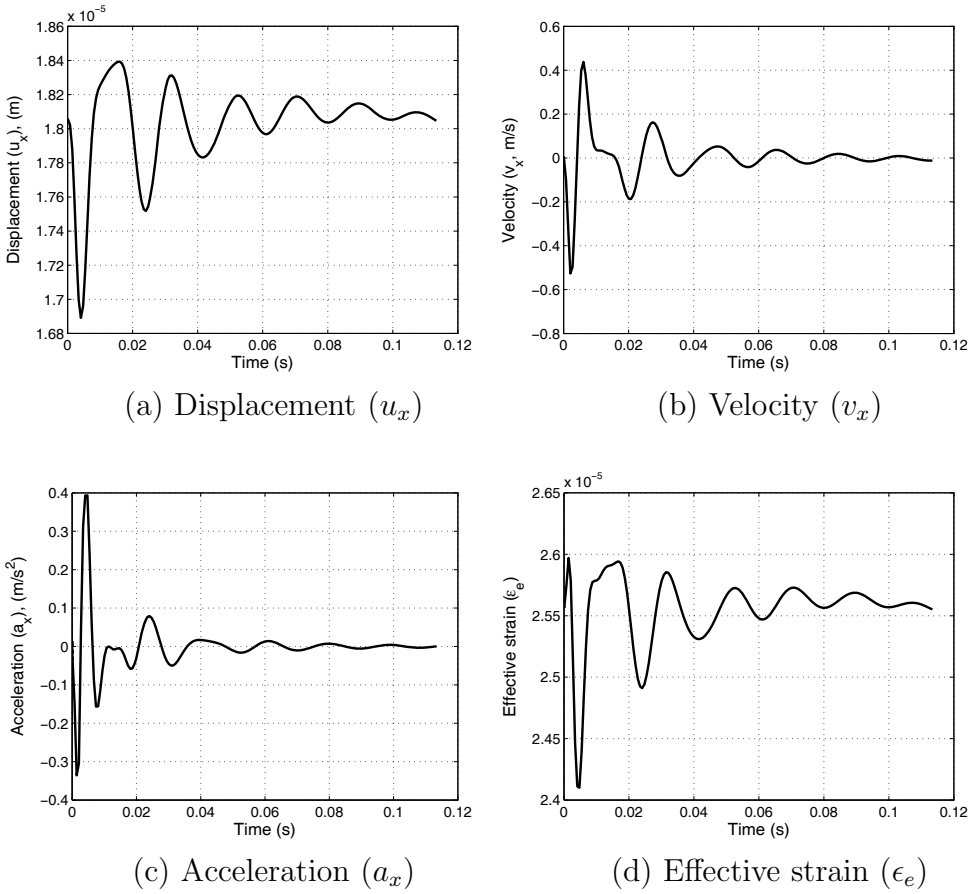

(a) Displacement (u_x) (b) Velocity (v_x)

(c) Acceleration (a_x) (d) Effective strain (ϵ_e)

Figure 4: Time history of vibrational responses (ICP = 1000 Pa)

response is, sensitivity is defined. It is found that some vibrational responses are more sensitive than the others to the change of intracranial pressure. The displacement and the velocity are the most sensitive. The acceleration and the effective strain are less sensitive. The fundamental frequency is the most insensitive to ICP change. The results from this study may be used as a base for developing a non-invasive procedure for evaluating intracranial pressure.

ACKNOWLEDGEMENTS

The research fund awarded by Manitoba Medical Service Foundation (MMSF) in 2008 for supporting the reported research is gratefully acknowledged.

References

[1] W. Goldsmith. The state of head injury biomechanics: past, present, and future. Part 1. *Critical Reviews in Biomedical Engineering*, 29:441–600, 2001.

[2] Y. Luo, Q. Zhang, and M. R. Del Bigio. Recent progress in application of FEM in study of non-penetrating brain injuries. *Advances in Theoretical and Applied Mechanics*, 1:225 – 240, 2008.

[3] R. Allen. Intracranial pressure: a review of clinical problems, measurement techniques and monitoring methods. *Journal of Medical Engineering and Technology*, 10:299 – 320, 1986.

[4] M. Stevanovic, G.R. Wodicka, J.D. Bourland, G.P. Graber, K.S. Foster, G.C. Lantz, W.A. Tacker, and A. Cymerman. The effect of elevated intracranial pressure on the vibrational response of the ovine head. *Annals of Biomedical Engineering*, 23:720 – 727, 1995.

[5] T. A. Whitman, G. R. Wodicka, M. T. Morgan, and J. D. Bourland. Measurement and modeling of the vibrational response of the ovine head as it relates to intracranial pressure. In *Ann. Int. Conf. of the IEEE Engng. in Medicine and Biology - Proceedings*, volume 2, pages 493 – 494, Amsterdam, Neth, 1996.

[6] V. Kostopoulos, E.E. Douzinas, E.M. Kypriades, and Y.Z. Pappas. A new method for the early diagnosis of brain edema/brain swelling. an experimental study in rabbits. *Journal of Biomechanics*, 39:2958–2965, 2006.

[7] P.C. Lauterbur. Image formation by induced local interactions: examples employing nuclear magnetic resonance. *Nature*, 242(5394):190 – 191, 1973.

[8] S. C. R. Williams. Nuclear magnetic resonance imaging. *Nuclear Magnetic Resonance*, (24):444 – 449, 1995.

[9] R. Muthupillai, D.J. Lomas, P.J. Rossman, J.F. Greenleaf, A. Manduca, and R.L. Ehman. Magnetic resonance elastography by direct visualization of propagating acoustic strain waves. *Science*, 269:1854 – 1857, 1995.

[10] M. A. Green, L. E. Bilston, and R. Sinkus. *In vivo* brain viscoelastic properties measured by magnetic resonance elastography. *NMR in Biomedicine*, 21:755 – 764, 2008.

[11] S. A. Kruse, G. H. Rose, K. J. Glaser, A. Manduca, J. P. Felmlee, C. R. Jack Jr., and R. L. Ehman. Magnetic resonance elastography of the brain. *NeuroImage*, 39:231–237, 2008.

[12] E.E.W. Van Houten, M.M. Doyley, F.E. Kennedy, K.D. Paulsen, and J.B. Weaver. A three-parameter mechanical property reconstruction method for MR-based elastic property imaging. *IEEE Transactions on Medical Imaging*, 24:311 – 324, 2005.

[13] M.D. Gilchrist and D. O'Donoghue. Simulation of the development of frontal head impact injury. *Computational Mechanics*, 26:229 – 235, 2000.

[14] G. Dassios, M.K. Kiriakopoulos, and V. Kostopoulos. On the sensitivity of the vibrational response of the human head. *Computational Mechanics*, 21:382–388, 1998.

[15] S.W. Gong, H.P. Lee, and C. Lu. Computational simulation of the human head response to non-contact impact. *Computers and Structures*, 86:758–770, 2008.

[16] O. C. Zienkiewicz, R. L. Taylor, and J. Z. Zhu. *The Finite Element Method: Its Basis and Fundamentals*. Elsevier Butterworth-Heinemann, 2005.

[17] Y. Luo. A Nearest-Nodes Finite Element Method with Local Multivariate Lagrange Interpolation. *Finite Elements in Analysis and Design*, 44:797–803, 2008.

[18] W. Goldsmith and K. L. Monson. The state of head injury biomechanics: past, present, and future. Part 2: Physical experimentation. *Critical Reviews in Biomedical Engineering*, 33:105–207, 2005.

[19] J.L. Davis. *Wave Propagation in Solids and Fluids*. Springer-Verlag, 1988.

[20] K. J. Bathe. *Finite Element Procedures*. Prentice-Hall, Englewood Cliffs, 1996.

Received: October, 2009